Time reversal of ultrafast waveforms by wave mixing of spectrally decomposed waves

Dan Marom, Dmitriy Panasenko, Rostislav Rokitski, Pang-Chen Sun, and Yeshaiahu Fainman

Department of Electrical and Computer Engineering, University of California, San Diego, 9500 Gilman Drive,
La Jolla, California 92093-0407

Two different realizations of time-reversal experiments of ultrafast waveforms are carried out in real time by use of four-wave mixing arrangements of spectrally decomposed waves. The first, conventional, method is based on phase conjugation of the waveform's spectrum and achieves time reversal of real amplitude waveforms. The second arrangement of the spectrally decomposed waves spatially inverts the waveform's spectrum with respect to the optical axis of the processor and achieves true time reversal for complex-amplitude ultrafast waveforms. We compare and contrast these two real-time techniques. © 2000 Optical Society of America
OCIS codes: 320.0320, 320.5540, 320.7110, 070.4340, 190.5040, 190.4380.

Time reversal of ultrafast waveforms has been demonstrated by use of several techniques, primarily spectral hole burning and photon echo in inhomogeneously broadened resonant absorbers[1–3] as well as time-domain holography and spectral holography.[4,5] Similarly, four-wave mixing with ultrashort pump pulses can be applied to perform time reversal.[6] These techniques generate exact time reversal if the temporal waveforms are real, as they are based on phase conjugation of the spectral information.[6,7] In this Letter we report the generation of true time reversal for complex-amplitude ultrafast waveforms by inversion of the spectral information of the signal about the center frequency. We perform the two time-reversal techniques—conventional spectral phase conjugation (SPC) and the novel spectral information inversion (SI)—by wave mixing four spectrally decomposed waves, utilizing cascaded processes in a $\chi^{(2)}$ nonlinear crystal. The unique attributes of our approach include instantaneous (femtosecond-scale) response time, high conversion efficiency, and long time window.

The spectral information exchange takes place in a spectral processing device (SPD), in which the temporal frequency components of the ultrafast waveforms are spatially dispersed. For real-time generation of the time-reversal waveforms, we utilize a nonlinear wave mixing process based on an arrangement that employs four-wave mixing by means of cascaded second-order nonlinearities (CSN's) in a $\chi^{(2)}$ medium. In contrast to that of the recently demonstrated spatial–temporal processor,[8] the arrangement in these experiments consisted of wave mixing spectrally decomposed waves (SDW's). The CSN arrangement consists of a frequency-sum process followed by a frequency-difference process that satisfies the type II noncollinear phase-matching condition. We introduce three ultrafast waveforms into the SPD: a complex-amplitude temporal information waveform and two transform-limited ultrashort pulses to serve as reference pulses (see Fig. 1). In the SI arrangement case, the spectral decompositions of the ultrafast waveforms are spatially dispersed in opposite directions

by diffraction from the grating's $+1$ and -1 orders at the SPD's input. SDW's U_1, U_2, and U_3 of the signal waveform $s(t)$ and the two reference pulses $r(t)$ in the high-resolution limit are given by[8]

$$U_1(x';t) = w\!\left[-\frac{ct}{\alpha}\right]\exp\!\left(j\,\frac{\omega_0 x' t}{\alpha f}\right)S\!\left(\frac{\omega_0 x'}{\alpha f}\right), \qquad (1)$$

$$U_2(x';t) = w\!\left[\frac{ct}{\alpha}\right]\exp\!\left(-j\,\frac{\omega_0 x' t}{\alpha f}\right)R\!\left(-\frac{\omega_0 x'}{\alpha f}\right), \qquad (2)$$

$$U_3(x';t) = w\!\left[-\frac{ct}{\alpha}\right]\exp\!\left(j\,\frac{\omega_0 x' t}{\alpha f}\right)R\!\left(\frac{\omega_0 x'}{\alpha f}\right), \qquad (3)$$

where $S(\,)$ and $R(\,)$ are the spectra of $s(t)$ and $r(t)$, respectively, $w[\,]$ is the input spatial mode profile on the diffraction grating (Fig. 1), α is the grating's angular dispersion parameter, f is the lens's focal length, ω_0 is the center frequency of the ultrafast waveforms, and c is the speed of light. For simplicity, we dropped the spatial separation by D of the input pupils of the beams (necessary to satisfy the noncollinear phase-matching condition in the Fourier plane). The spectrum of wave U_2 is inverted with respect to the spectra of U_1 and U_3 as a result of the opposite directions of spatial dispersion and a temporal carrier term, $\exp(j\omega_0 t)$. The frequency-sum process mixes the SDW's U_1 and U_2,
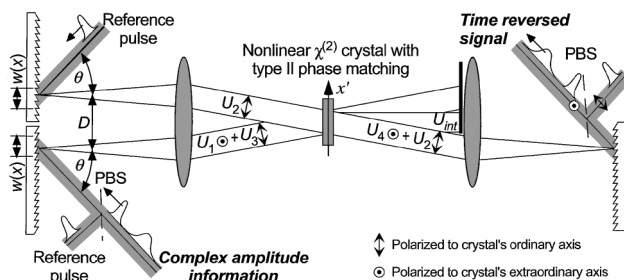
Fig. 1. Experimental setup for true time reversal of complex amplitude waveforms by four-wave mixing of mutually inverted SDW's by CSN. PBS's, polarizing beam splitter.

generating an intermediate wave $U_{int} \propto \chi^{(2)}U_1U_2$. Because of the energy of conservation principle and the opposite spatial dispersions, the intermediate wave is quasi-monochromatic at every spatial location x'.[9]

The spectral information from the input temporal signal is preserved in the wave-mixing process and is converted into spatial modulation of the intermediate wave. These two desirable properties were used in the past for ultrafast waveform imaging.[9] The second nonlinearity in the cascade is a frequency-difference process that mixes U_{int} with the SDW of U_3, generating an output SDW $U_4 \propto \chi^{(2)}U_{int}U_3{}^*$. Substituting Eqs. (1)–(3) yields output SDW

$$U_4(x';t) \propto \exp\left(-j\,\frac{\omega_0 x't}{\alpha f}\right)S\left(\frac{\omega_0 x'}{\alpha f}\right)R\left(-\frac{\omega_0 x'}{\alpha f}\right)$$

$$\times R^*\left(\frac{\omega_0 x'}{\alpha f}\right), \tag{4}$$

where we have dropped the time windows imposed by the input pupils, $w[\pm ct/\alpha]$, for brevity. The spectral information in $S()$ is inverted with respect to the spatial dispersion direction, which is defined by the sign of the exponent term [cf. also Eq. (2)], thus achieving our goal of spectral information inversion. The SDW U_4 is recomposed by the second grating of the SPD to yield the output temporal waveform $y(t) = s(-t) \otimes r(t) \otimes r^*(t)$, where $\otimes$ denotes the convolution operator. As $r(t)$ is a transform-limited reference pulse, the conjugation term in the last equation can be dropped. The generated output signal is therefore proportional to the time-reversed signal waveform convolved twice with a reference pulse, broadening the temporal features of the signal waveform. The SPD's time window of operation is defined by the input pupils of the interacting waves and not by the crystal dimensions, as in time-domain four-wave mixing.[6] Therefore the processor's time window can be tailored to the desired application, usually in the several-picosecond range.

Our second time-reversal experiment was based on generating the phase conjugate of the signal spectrum, implementing a real-time spectral processing version of the technique reported in Ref. 5. The arrangement of Fig. 1 was modified such that the three waves enter the SPD from the same direction, utilizing the same diffraction order, and the signal information wave is used to initiate the downconversion process. The resultant SDW in this arrangement is given by

$$\hat{U}_4(x';t) \propto \exp\left(j\,\frac{\omega_0 x't}{\alpha f}\right)S^*\left(\frac{\omega_0 x'}{\alpha f}\right)R\left(\frac{\omega_0 x'}{\alpha f}\right)$$

$$\times R\left(\frac{\omega_0 x'}{\alpha f}\right), \tag{5}$$

where again we have dropped the time windows from the expression and added the circumflex to U_4 to distinguish the SDW's of relations (4) and (5). We find that the output temporal waveform in this case is $\hat{y}(t) = s^*(-t) \otimes r(t) \otimes r(t)$. The only difference in the two resultant time-reversed waveforms, $\hat{y}(t)$ and $y(t)$, is

the conjugation operation on the signal waveform. If one constrains the information signals to contain only real data, the SI and SPC time-reversal results are equivalent. For complex amplitude information, the two results will differ.[6]

The ultrafast signals in our experiments were detected and analyzed with a real-time ultrafast waveform imaging system.[9] The imaging system produces a quasi-monochromatic wave in a three-wave mixing process within a SPD, mixing the SDW of the ultrafast signal waveform and an inverted SDW of a reference pulse [same forms as Eqs. (1) and (2), respectively]. The generated wave is spatially modulated by the spectrum of the signal waveform. A spatial Fourier transform to the image plane of the SPD generates a spatial signal that is proportional to the complex amplitude of the ultrafast waveform. In the case of an input signal waveform consisting of a chirped pulse, the output field will carry a quadratic phase function in space. We can measure this spatial quadratic phase modulation by displacing the observation plane away from the image plane and finding the location where the wave is focused to its tightest spot (as the quadratic phase is compensated for by free-space propagation). From the direction and amount of displacement, the magnitude and sign of the quadratic phase term of the ultrafast waveform that is imaged are deduced.

Both time-reversal experiments were performed in a SPD consisting of 600-line/mm blazed gratings and lenses of 375-mm focal length, with a 2-mm long β-barium borate crystal placed in the Fourier plane. The three input waveforms were derived from a single ultrashort pulse (generated from a Ti:sapphire ultrashort pulse oscillator combined with a regenerative amplifier) with 100-fs duration, a center wavelength of 800 nm, and an energy level of <1 mJ. The signal waveform contained 10% of the optical power; the remaining 90% was used for the reference pulses (which serve as pump waves) to maximize the conversion efficiency. To demonstrate the true time-reversal property of complex amplitude waveforms by wave mixing oppositely dispersed SDW's we used a complex waveform consisting of a transform-limited pulse followed by a positively chirped pulse. The waveform was generated by an unequal-arm Mach–Zehnder interferometer with a grating pair placed in one arm. Let the complex amplitude signal waveform be defined as $s(t) = a_1(t) + a_2(t - t_0)\exp[j\phi_2(t - t_0)^2]$, where $a_1(t)$ and $a_2(t)$ are the real signal envelopes and ϕ_2 defines the quadratic phase term [see the schematic curve in Fig. 2(a)]. In the SI case we expect the time-reversed signal to preserve the quadratic phase sign, i.e., $y(t) \propto s(-t) = a_1(-t) + a_2(-t - t_0)\exp[j\phi_2(-t - t_0)^2]$ [Fig. 2(b)], whereas for time reversal obtained from the SPC method the quadratic phase term reverses its sign: $\hat{y}(t) \propto s^*(-t) = a_1(-t) + a_2(-t - t_0)\exp[-j\phi_2(-t - t_0)^2]$ [Fig. 2(c)]. Figure 3 shows the experimental results of ultrafast waveform imaging for the input information signal $s(t)$ and the two time-reversed waveforms $y(t)$ and $\hat{y}(t)$, illustrating the difference between the two techniques for generating time-reversed waveforms. The input temporal signal consists of a
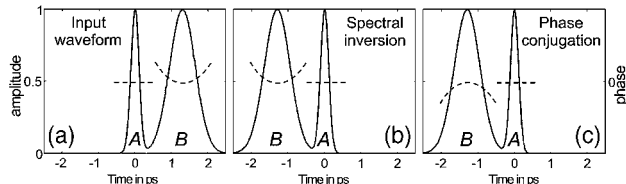
Fig. 2. Schematics of (a) the complex amplitude input waveform and of time inversed waveforms by (b) spectral inversion and (c) phase conjugation, illustrating the difference in the two time-reversal techniques. Solid curves, signal magnitude; dashed curves, signal phase.
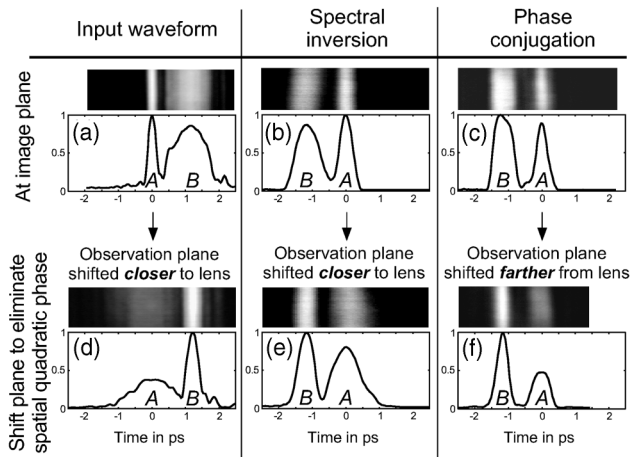
Fig. 3. Spatial images and extracted termporal information of ultrafast waveforms in the time-reversal experiments: (a) input waveform; time reversed waveforms by (b) spectral inversion and (c) phase conjugation. Both time-reversal methods interchange the locations of the pulses, but the SI preserves the complex-amplitude information, as determined by the quadratic phase of pulse B. Displacing the image plane closer to [(d) and (e)] or farther from [(f)] the lens compensates for positive or negative quadratic phase, respectively.

transform-limited pulse followed by a chirped pulse [Fig. 3(a)]. Displacing the observation plane closer to the Fourier transform lens cancels the quadratic phase and focuses the chirped pulse to its tightest spot [Fig. 3(d)]. Both time-reversal methods transposed the locations of the two pulses [Figs. 3(b) and 3(c)]. The SI reversal experiment preserved the quadratic phase sign information, as is evident from the chirped pulse focusing closer to the lens [Fig. 3(e)], whereas the SPC signal reversed the sign of the quadratic phase [Fig. 3(f)]. Wave mixing of mutually inverted SDW's has the additional benefit of better phase matching in the wave-mixing process for different temporal frequency components, as group-velocity mismatch is spatially compensated for.[10] Therefore the SI signal supported a broader bandwidth, resulting in higher-resolution spatial images (compare the relative widths of the transform-limited pulse and the chirped pulse in the SI and SPC cases). The conversion efficiency of the wave-mixing process was 14%, defined by the ratio of the powers of the time-reversed waveform to that of the input signal waveform. The high conversion efficiency is attributed to the effective energy transfer of the CSN process.

In summary, we have introduced and experimentally demonstrated the SDW mixing approach to time reversal of ultrafast waveforms, which is operated in real time on a single-shot basis with high conversion efficiency because of the CSN process. The method was applied for time-reversal transformations by SI and SPC. Other signal processing operations, such as convolution and correlation, can be performed on ultrafast waveforms with this real-time technique, which may be desirable for optical communication applications. It has been shown that true time reversal of complex-amplitude ultrafast waveforms is achieved by spectral information inversion. The complex-amplitude waveform was reversed in time, as is evident by the chirped pulse's maintaining the quadratic phase information. Spectral holography was used in the past for time reversal by SPC[5] (albeit not in real time) and can be modified to perform SI. Referring to Fig. 1, one can record the stationary interference signal of SDW's U_1 and U_3 (as is done in conventional spectral holography). To achieve spectral information inversion, let the readout wave be the SDW U_2, with the inverted spatial dispersion direction. Alternatively, one can physically rotate the hologram by 180° about the optical axis before conventional readout. The spatial information recorded in the x' coordinate system is converted to the $-x'$ system, resulting again in spectral information inversion.

References

1. N. W. Carlson, L. J. Rothberg, A. G. Yodh, W. R. Babbitt, and T. W. Mossberg, Opt. Lett. **8,** 483 (1983).
2. A. Rebane, J. Aaviksoo, and J. Kuhl, Appl. Phys. Lett. **54,** 93 (1989).
3. V. L. da Silva, Y. Silberberg, J. P. Heritage, E. W. Chase, M. A. Saifi, and M. J. Adrejco, Opt. Lett. **16,** 1340 (1991).
4. L. H. Acioli, M. Ulman, E. P. Ippen, J. G. Fujimoto, H. Kong, B. S. Chen, and M. Cronin-Golumb, Opt. Lett. **16,** 1984 (1991).
5. A. M. Weiner, D. E. Leaird, D. H. Reitze, and E. G. Paek, IEEE J. Quantum Electron. **28,** 2251 (1992).
6. D. A. B. Miller, Opt. Lett. **5,** 300 (1980).
7. P. Saari, R. Kaarli, and A. Rebane, J. Opt. Soc. Am. B **3,** 527 (1986).
8. D. M. Marom, D. Panasenko, P.-C. Sun, and Y. Fainman, Opt. Lett. **24,** 563 (1999).
9. P.-C. Sun, Y. Mazurenko, and Y. Fainman, J. Opt. Soc. Am. A **14,** 1159 (1997).
10. A. M. Kan'an and A. M. Weiner, J. Opt. Soc. Am. B **15,** 1242 (1998).